CHAPTER 9

ELECTRICAL CONDUCTIVITY MEASUREMENTS

Contents

9.1 INTRODUCTION

The defect chemistry of crystalline solids, in general, can be understood by the study of their electrical properties. Unlike metals and semiconductors where electrons are the charge carriers, in poor and semi-insulators the prime factors contributing to their electrical conductivity are the crystal defects such as isolated cations or anions (Schottky defects), cation substitutional impurities, cation vacancy-cation impurity complexes, vacancy pairs, cationic interstitials (Frenkel defects), colour centres, and on many occasions the stacking faults, mozaics, etc. The literature shows a great interest in the defect chemistry of ternary compounds. Many authors have applied the ideas of Schmalzried (1,2) and Kröger and co-workers (3,4) to the defect chemistry of certain specific compounds.

Eventhough the available literature supplies some information about the electrical conductivity of rare-earth tungstates such as $Nd_2(WO_4)_3$ and $EuWO_4$ (5-7), the conduction mechanism being explained in terms of electrons or holes, polarons and impurities, a meagre literature is recorded about that of Scheelite compounds. In 1975, Petrosyan et al (8) have simply mentioned the

characteristic values of the conductivity at 20°C for $CaMoO_4$, $BaMoO_4$, $SrMoO_4$, Na_2MoO_4, while studying the phase diagrams of the systems Na_2MoO_4-$MMoO_4$ (M= Ca, Ba, Sr and Na). Later Van Loo (9) and Groenink (10) made extensive studies on electrical conductivity of $PbMoO_4$ and $PbWO_4$. Lal et al (11) have investigated the electrical conductivity of $CaWO_4$ crystals in attribution to the oxygen vacancies and polarons. An earlier study (12,13) of the molybdates of calcium and strontium in the oxygen pressure range 0.01 - 1.0 atm. has shown that these oxide phases possess mixed electron hole-ion conductivity. It was suggested that the predominant defects were oxygen and molybdenum vacancies. Rigdon and Grace (14) studied the electrical conductivity of $CaWO_4$ at 900-1300°C and partial pressure of oxygen from 10^{-9} to 10^{-14} atm. The defect structure was interpreted in terms of oxygen vacancies and interstitials. The authors did not take into consideration that molybdenum and tungsten show relatively high mobility in molybdates and tungstates respectively (15). Petrov and Kofstad (16) reported the electrical conductivity and ionic transport number of $CaMoO_4$ as a function of the partial pressure of oxygen $1-10^{-18}$ atm. at 750, 800 and 850°C.

The present chapter comprises the results of a study of the electrical conductivity of $CaMoO_4$ measured in this laboratory in the temperature range 4C-500°C (or 313-773 K) in air atmosphere.

9.2 EXPERIMENTAL DETAILS

The single crystals of calcium molybdate grown (Chapter 4) by flux cooling method, using LiCl as flux, were used. For the purpose of electrical conductivity measurements the grown crystals were ground to fine powder using ball-mill and then pressed into the form of circular pellets of 10 mm diameter and 2 mm thickness, using a stainless-steel die and a hand-operated hydraulic press at a pressure of 9.84×10^2 kg . cm^{-2}. On the other hand, the platy crystals employed for the study were about 1 mm thick with surface area of about 0.04 cm^2. The measurements were carried out using the two electrode method. The crystal or the pellet, as the case may be, was annealed, cleaned and dried before the measurements. The specimen was mounted inbetween two flat stainless-steel circular parallel electrodes of a specially designed conductivity cell shown schematically in Fig. 8.1 (Chapter 8). Both the upper and the lower cylindrical tubes of the cell can be screwed in for proper contact of the

specimen, under study, with the electrodes. Experiments were also performed using silver painted electrodes. For the study of the effect of temperature on the conductivity, the cell was enclosed in a specially-built resistance heated furance and the temperature was raised slowly by regulating the power through 230 V, 50 Hz mains using a dimmerstat. To monitor the actual temperature of the specimen, a Pt-Pt. 10 % Rhodium thermocouple was used.

The electrical resistance was measured using a BPL (India) Million Megohmmeter Model RM 160 MK and the results were reproducible within $\pm$ 5 % accuracy. The total experimental set up is shown in Fig. 9.1.

9.3 RESULTS AND DISCUSSION

9.3.1 D. C. conductivity

The electrical conductivity in solids is usually explained using the band theory of solids, according to which the variation of σ and θ in intrinsic semiconducting solids are given by the following expressions : (17)

$$\sigma_{in} = 2e\left[(2\pi kT)/h^2\right]^{3/2} (m_e m_h)^{3/4} (\mu_e + \mu_h) \exp\left[-Eg/2kT\right] \qquad (9.1)$$

or

$$\sigma_{in} = \sigma_o (T) \exp (- Eg/2kT) \qquad (9.2)$$

where

$$\sigma_o (T) = 2 e [(2\pi kT)/h^2]^{3/2} (m_e m_h)^{3/4} (\mu_e + \mu_h) \qquad (9.3)$$

and,

$$\theta = - \frac{E_g}{2e} \left(\frac{C-1}{C+1} \right) \frac{1}{T} - \frac{2k}{e} \left(\frac{C-1}{C+1} \right) - \frac{3k}{4e} \log_e (a) \qquad (9.4)$$

or $$\theta = \left(\frac{n}{T} \right) + K \qquad (9.5)$$

where $$n = - \frac{Eg}{2e} \left(\frac{C-1}{C+1} \right) \qquad (9.6)$$

$$K = - \left[\frac{2k}{e} \left(\frac{C-1}{C+1} \right) + \frac{3k}{4e} \log_e (a) \right] \qquad (9.7)$$

$$C = \frac{\mu_e}{\mu_h} , \quad a = \frac{m_e}{m_h}$$

k and h are Boltzmann and Plancks ccnstants, m_e, μ_e and m_h and μ_h are effective masses and mobilities of electron and hole respectively and Eg is the energy

band gap of the solid. Clearly, a plot of σ versus 1/T and θ versus 1/T should yield straight line under certain approximations.

The D. C. electrical conductivity, σ, studied in the temperature interval of 40-500°C (or 313-773 K) in air atmosphere has been found to be dependent upon the electrode materials used. There is a marked deviation in the absolute values of the conductivity when stainless-steel and silver painted electrodes are employed. Table 9.1 shows the values of σ for pelletised samples, using silver painted and stainless-steel electrodes. The reason for the discrepancy in the absolute values seems to be the non-ohmic contact or simple contact resistance in the electrode (metal) - insulator interface. Silver paint seems to give a better ohmic contact than the other electrode. The variation of ln σ versus 1/T for pellet and single crystalline specimens using stainless-steel electrodes are shown in Figs. 9.2 and 9.3 respectively. It is interesting to note that the nature of variation for both the samples is almost the same. The variation illustrated in Figs.9.2 and 9.3 exhibits two straight lines, following the relation

Table 9.1 Experimental values of σ of $CaMoO_4$ pellet, employing silver-paint and stainless steel electrodes at different temperatures

Temperature K	σ, $Chm^{-1}\ cm^{-1}$	
	Silver painted electrodes	Stainless-steel electrodes
1	2	3
383	3.35×10^{-11}	2.95×10^{-12}
393	3.86×10^{-11}	2.12×10^{-12}
413	4.55×10^{-11}	2.36×10^{-12}
423	4.90×10^{-11}	2.59×10^{-12}
433	7.07×10^{-11}	3.10×10^{-12}
453	9.09×10^{-11}	2.07×10^{-11}
463	1.21×10^{-10}	5.00×10^{-11}
483	3.18×10^{-10}	2.04×10^{-10}
493	7.27×10^{-10}	4.16×10^{-10}
513	3.74×10^{-9}	1.59×10^{-9}

1	2	3
523	5.09×10^{-9}	3.64×10^{-9}
533	1.20×10^{-8}	5.66×10^{-9}
543	3.50×10^{-8}	1.02×10^{-8}
553	3.70×10^{-8}	1.54×10^{-8}
573	5.50×10^{-8}	2.64×10^{-8}
583	8.50×10^{-8}	6.36×10^{-8}
593	1.27×10^{-7}	7.47×10^{-8}
603	2.11×10^{-7}	1.37×10^{-7}
613	3.18×10^{-7}	2.38×10^{-7}
623	6.94×10^{-7}	3.93×10^{-7}
633	9.10×10^{-7}	6.35×10^{-7}
643	1.49×10^{-6}	1.13×10^{-6}
653	2.11×10^{-6}	1.41×10^{-6}

$$\sigma = \sigma_o \exp\left(-\frac{E}{kT}\right) \qquad (9.8)$$

where σ_o is a constant, and E the activation energy.

9.3.2 Extrinsic and intrinsic conduction

The slow rate of decrease of σ with increase in the reciprocal temperature T, as seen from the curves, together with the low mobility of charge carriers and the ionic nature of $CaMoO_4$ lattice, points to a strong coupling of charge carriers with lattice ions. The initial linear variation of the two curves is seen to have been broken at a temperature, T_B = 430 K (Fig. 9.2, pellet) and T_B = 438 K (Fig. 9.3, crystal). Even though, in general, the molybdates are known to be less stable compounds compared to the tungstates (9), the differential thermogravimetric analysis (DTA) experiment (Chapter 5) fails to show any phase change in the studied temperature range and, in particular, at the temperature T_B. It may, therefore, be concluded that there exist two types of conduction, corresponding to the lower and the higher temperature regions. The temperature T_B may, however, be attributed to the transition of conduction contributed by different types of charge carriers.

The conductivity in the high temperature region is expressed by

$$\sigma = \sigma_{o_1} \exp\left(-\frac{E_1}{kT}\right) \qquad (9.9)$$

whence this conduction is due to one type of charge carriers, with

$$E_1 = \frac{1}{2} h_F + h_m \qquad (9.10)$$

where h_F is the energy of formation of Frenkel defects and h_m is the migration energy of the mobile specimen and σ_{o_1} is a pre-exponential constant.

At lower temperatures, the conductivity, as determined by the frozen-in defects, is given by

$$\sigma = \sigma_{o_2} \exp\left(-\frac{E_2}{kT}\right) \qquad (9.11)$$

where

$$E_2 = h_m \qquad (9.12)$$

and σ_{o_2} is another pre-exponential factor. Should the same carrier be mobile in the two temperature regions,

then the Frenkel defect formation energy h_F can be computed from the equations (9.10) and (9.12) as

$$2(E_1 - E_2) = h_F \qquad (9.13)$$

The activation energies E_1 and E_2, calculated from the slopes of each of the two curves from Figs. 9.2 and 9.3, are presented in Table 9.2. The two slopes in Figs. 9.2 and 9.3 can be attributed to the intrinsic conductivity at high temperatures ($>$ 440 K) and to the extrinsic conductivity at low temperatures ($<$ 440 K), both being independent of the specimen preparation history. The activation energy of the low temperature conductivity is lower than that of the high temperature region in both the cases, and the activation energy for the crystal is less than that of the pellet. Consequently, one expects a higher conductivity in the case of crystalline materials.

In ionic crystals like $CaMoO_4$, there are possibly two kinds of Frenkel defects accentuated by cations or anions moving into interstitial positions (18). By the motion of the interstitial ions and the vacant lattice points a current may be constituted.

Table 9.2 The values of activation energy and of Frenkel defect formation, in eV, for $CaMoO_4$

Temperature range	Energy	Pellet	Crystal
High-temperature region (Intrinsic)	E_1	1.40	1.08
Low-temperature region (Extrinsic)	E_2	0.65	0.066
	h_F	1.50	2.028

Since the ionic sizes of Ca^{2+} and MoO_4^{2-} are different, one expects a large difference in the energies required to put them into iterstitial positions. Hence, in such a crystal in which the current is due mostly to Frenkel defects, either the cations or anions only will be responsible for the conduction phenomena. It may be mentioned that the oxygen vacancies and oxygen interstitials are the majority of defects at higher temperatures in this type of crystals (19). The fact that Frenkel and anti-Frenkel disorders exist in lattices supports the formation of oxygen ion vacancies O_v^{2-} and interstitials O_i^{2-} by the reaction,

$$O^{2-} \rightleftharpoons O_v^{2-} + O_i^{2-}$$

Since there is not much difference between the pycnometric and X-ray densities (Chapter 5) of the flux-grown $CaMoO_4$ crystals, there may be present some concentration of Frenkel defects (20). Therefore, the conductivity in the intrinsic region is substantially due to oxygen vacancies.

At lower temperatures (below 440 K) the conductivity is governed by the mobile ions or lattice

defects. Only the small amount of Schottky defects that would be formed during its growth may be essentially responsible to contribute to this extrinsic conduction.

9.4 CONCLUSIONS

1. The variation in conductivity with temperature is found to depend on the type of electrodes employed for study.

2. Single crystal specimens and pelletised samples show distinct conductions, namely extrinsic and intrinsic, at lower and higher temperature regions, respectively.

3. In $CaMoO_4$, migration of the defects in the oxide sublattice probably contributes to the conductivity in the intrinsic region, while the extrinsic conductivity prevails on account of some sort of impurities.

REFERENCES

1. H. Schmalzried and C. Wagner. (1962)
Z. Phys. Chem. N. F., 31, 198.

2. H. Schmalzried. (1965)
Prog. Solid State Chem., 2, 265.

3. F. A. Kröger. (1973)
"Chemistry of Imperfect Crystals"
(North-Holland Publishing Company, 2, 826).

4. F. A. Kröger and H. J. Vink. (1956)
Solid State Phys., 3, 307.

5. H. B. Lal, N. Dar and Ashok Kumar. (1974)
J. Phys. C : Solid State Physics, 7,4335.

6. H. B. Lal and N. Dar. (1975)
J. Phys. C : Solid State Physics, 8, 2745.

7. H. B. Lal and N. Dar. (1977)
J. Phys. Chem. Solids, 38, 161.

8. Yu. G. Petrosyan, E. V. Tkachenko and
V. M. Zhukovskii. (1975)
Inorg. Mater., 11, 1381.

9. W. Van Loo. (1975)
J. Solid State Chem., 14, 359.

10. J. A. Groenink. (1979)
Ph. D. Thesis, State University, Utrechet.

11. H. B. Lal, N. Dar and Ashok Kumar. (1974)
Ind. J. Pure and Appl. Phys., 12, 539.

12. V. Zhukovsky and A. Petrov. (1972)
Proc. Acad. Sci. USSR, Inorg. Mater., 8, 518.

13. V. Zhukovsky and A. Petrov. (1973)
J. Appl. Chem. USSR, 46, 2159.

14. M. A. Rigdon and R. E. Grace. (1973)
J. Amer. Ceram. Soc., 56, 475.

15. V. Zhukovsky, E. Tkachenko, A. Zhukovskaja and N. Veselova. (1976)
Collection of papers of the Ural State University on "Physics of Metals and Their Compounds", 49.

16. Alexander Petrov and Per Kofstad. (1979)
J. Solid State Chem., 30, 83.

17. T. C. Herman and J. M. Honing. (1976)
"Thermoelectric power and thermodynamic effects and applications" (New York : McGraw Hill), 142.

18. N. F. Mott and R. W. Gurney. (1957)
"Electronic Processes in Ionic Crystals" (Clarendon Press, Oxford), 41.

19. M. A. Rigdon and R. E. Grace. (1974)
J. Amer. Ceram. Scc., 57, 245.

20. N. N. Greenwood. (1970)
"Inoic Crystals Lattice Defects and Non-stoichiometry" (Butterworth and Co.),77.

Fig. 9.1 Experimental set-up for conductivity measurements.

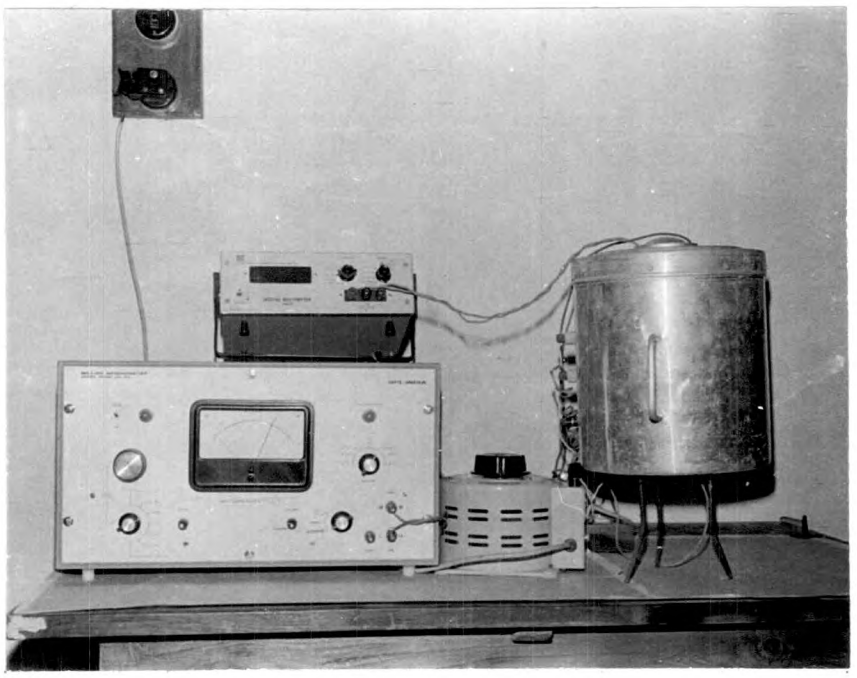

Fig. 9.1

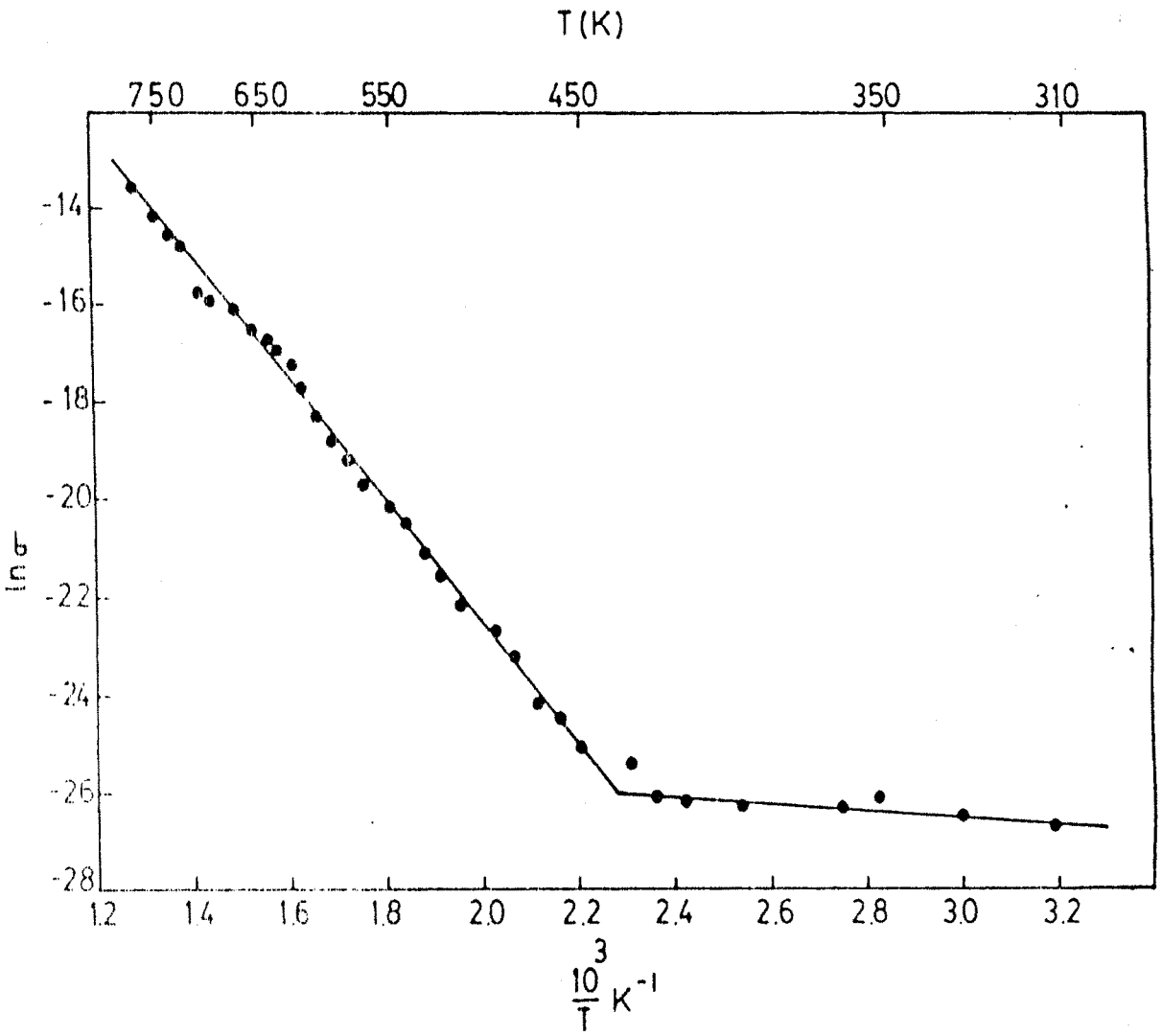

Fig.9.2 Graphical plot of ln σ versus 1/T for a pellet.

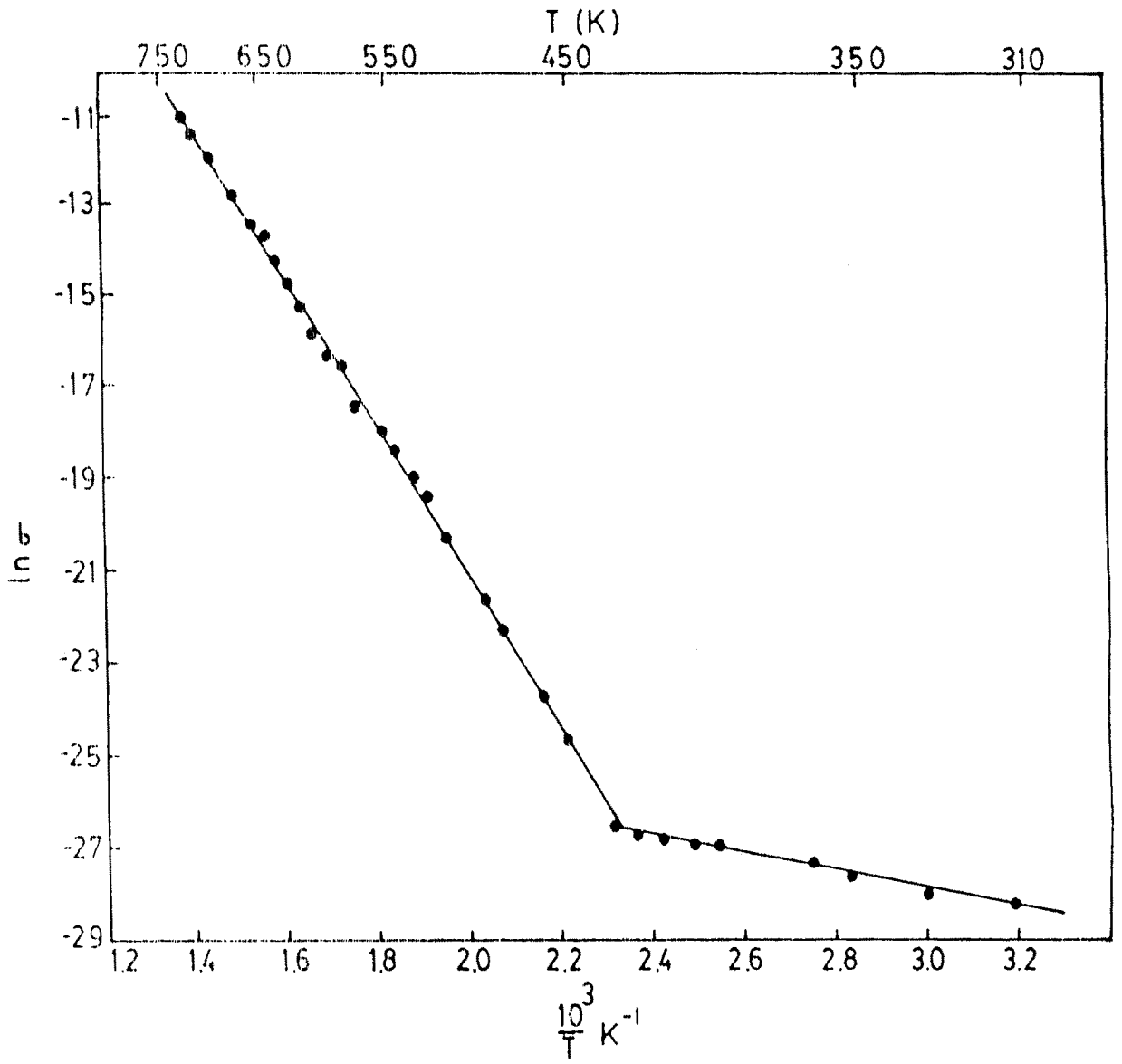

Fig. 9.3 Graphical plot of ln σ versus 1/T for a crystal.